fire

MDPI

Article

Quantifying the Effectiveness of a Mesh in Mitigating Burning Capabilities of Firebrand Shower

Ahmad Sharifian Barforoush * and Matthew du Preez

School of Engineering, Faculty of Health, Engineering and Science, University of Southern Queensland, 487-535 West St, Darling Heights, Toowoomba, QLD 4350, Australia
* Correspondence: sharifia@usq.edu.au

Abstract: The broad aim of this research is to quantify the effectiveness of fences made of metal mesh around buildings in mitigating risks associated with firebrand showers created in wildland fires. This paper aims to (1) quantify the effectiveness of a mesh complying with Australian Standard 3959:2018 against firebrand showers and (2) identify behaviors of firebrands interacting with the mesh. The study was conducted using Red Gum and Cypress Pinewood firebrands inside a wind tunnel at 40 km/h with and without a mesh present for a total of 50 experiments. Two types of effectiveness were defined using the number of holes and their area burnt by the firebrand. The results show the mesh was highly effective against both large and small firebrands except for some long needle shape firebrands. The results are aligned with AS 3959:2018 and show an effectiveness ratio of the mesh in the range 93.2–98.8% for Red Gum and Cypress Pine firebrands at a wind speed of 40 km/h. It was documented that firebrands in interaction with the mesh show one or a combination of eight different mechanisms: passing, stopping, splitting, shattering, pausing, bouncing, slipping and wandering.

Keywords: wildfire; mesh; firebrand; red gum; cypress pine; wind tunnel

Citation: Sharifian Barforoush, A.; du Preez, M. Quantifying the Effectiveness of a Mesh in Mitigating Burning Capabilities of Firebrand Shower. *Fire* **2022**, *5*, 150. https://doi.org/10.3390/fire5050150

Academic Editor: Tiago Miguel Ferreira

Received: 26 August 2022
Accepted: 24 September 2022
Published: 28 September 2022

1. Introduction

Global warming has increased the length and intensity of the fire seasons and is driving worsening wildfires. Many protocols, standards and guidelines have been developed to minimize the impact of wildfires on the human habitat. Among those standards and guidelines is AS 3959:2018 which specifies requirements for the construction of buildings in wildfire-prone areas in Australia to improve their resistance to burning firebrands. According to the standard, screens with a maximum aperture of 2.0 mm shall be fitted to the openings of doors and windows. The standard does not mandate utilizing fencing and screen walls to improve house survivability beyond the base levels provided in the standard. However, the standard acknowledges that the use of screens may reduce the exposure of a building to firebrand attacks and other potential fire sources such as adjacent buildings [1].

Previous studies show that metal screens are effective in mitigating the risk of firebrand attacks [2–6] but not all firebrands quench in the presence of screens. They burn until they fit through the screens [2] or shatter into smaller pieces when they hit the screen and produce secondary firebrands which are smaller than approaching firebrands [5]. Larger firebrands and flaming firebrands show greater potential in inducing ignition on the fuel beds in comparison with smaller and glowing firebrands [7]. All previous studies were conducted using horizontal fuel beds. The fuel beds were placed at different distances from the screens to capture landing firebrands [8–10] or the firebrands were directed on the fuel beds by means of fine meshes [8] or walls [4].

The aim of this research is to quantify the effectiveness of fences made of metal mesh around buildings in mitigating wildfire risks. Previous studies show that the flying distance of firebrands depends on parameters such as size, mass, shape, density, porosity, temperature, vegetation species, combustion rate and state of combustion of firebrands [10–12]. The

glowing surface area of firebrands and their number are important parameters to determine whether ignition of fuel beds occurs [8]. Therefore, the landing firebrands collected by pans at a relatively short distance may not possess the same characteristics as long-distance flying firebrands and may not represent the mean characteristic of firebrands penetrating the mesh. In addition, the characteristics of firebrands collected a long distance from the mesh may be unrepresentative of the time of penetration due to the continuation of burnings. Furthermore, the firebrands directed to horizontal fuel beds may shatter into smaller pieces which will impact the accuracy of measurements.

The specific objectives were to: (a) Understand the mechanisms of the firebrand-mesh interaction and (b) quantify the impact of the mesh on the burning capabilities of the firebrand shower. To the best of the authors' knowledge, this is the first study to quantify the effectiveness of the mesh against flying firebrands and document all the behaviours of the firebrands interacting with the mesh.

In this work, Cypress Pine and Red Gum firebrands were generated to assess the impact of the type of vegetation. Firebrands passed through a mesh and the burning capabilities of flying firebrands were quantified by counting the number of the holes generated by firebrands and measuring their sizes on a highly sensitive thin plastic sheet placed vertically 2 m from the screen. All experiments were conducted with and without mesh to compare the number of burnt holes and their areas on the plastic sheet.

In this work, the performance of the screen against a firebrand shower at a wind speed of about 40 $\pm$ 2 km/h was assessed.

All experiments were conducted in the Southern hemisphere summer (December–March) in a relatively warm temperature with low to medium relative humidity. The behavior of firebrands and accuracy of the experiments were controlled at 4 points which were the furnace, the test section, the exit of the ESS and the plastic sheet.

2. Materials and Methods

2.1. Ember Shower Simulator

The experiments were conducted using a wind tunnel specifically designed and manufactured to generate a firebrand shower. The Ember Shower Simulator (ESS) shown in Figure 1 generates a firebrand shower at wind speeds up to 16 m/s [5]. A fan on the right-hand side draws air into the ESS. A flap directs a fraction of the airflow towards the furnace where vegetation is burned to generate firebrand. The upward flow of hot air in the furnace and the wind entering the furnace cause the firebrands to move upwards and into the wind tunnel. The wind speed in the furnace is controlled by the distance of the fan from the wind tunnel and the height of the flap. The generated firebrand from the furnace mixes with air which flows over the flap, through the test section and exits the ESS. In this study, a plastic sheet holder was attached to the end of the wind tunnel 2 m downstream of the mesh holder. The details of the plastic sheet holder are presented in Section 2.3.

The performance of the screen against the firebrand shower was assessed at an average wind speed of 40 km/h. The flow experiences velocity non-uniformity due to the flap and the mixing of hot air from the furnace with cold air directed over the flap. Based on the velocity measurements at nine points (three heights each sampled at three points spaced horizontally equidistantly), it was found that the maximum non-uniformity occurs when the highest flap of 150 mm was used, and without mesh placed at the test section. In that case, the standard deviation (or the coefficient of variation) was 9.5% and 6.3% at the inlet and outlet to the test section, respectively. Further details on the non-uniformity of flow can be found in [5].

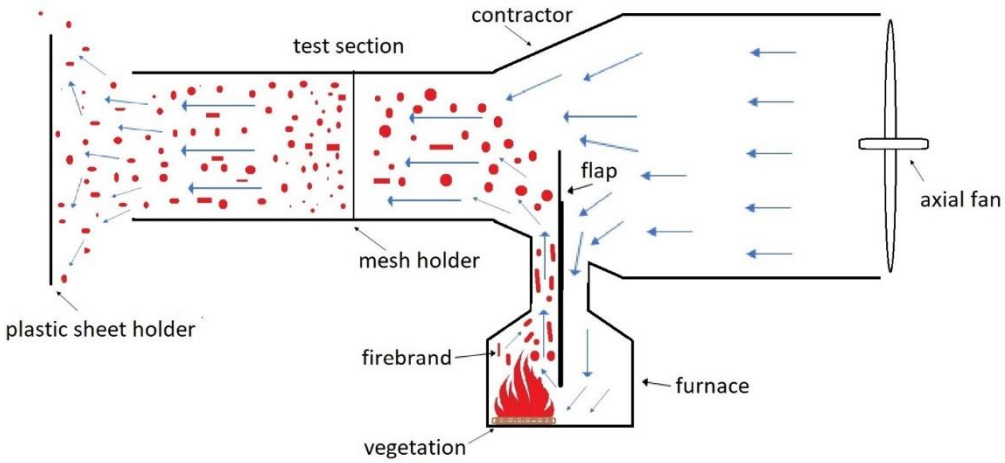

Figure 1. Schematic of the ESS.

2.2. Vegetation

Firebrands cause spot fires when they land on fuel beds. Previous studies show that any burning vegetation can act as firebrands [13,14]. In practice, a non-artificial firebrand shower is a combination of firebrands sourced from various types of vegetation both in glowing/smoldering or flaming states. However, only firebrands that burn and fly a long distance represent a significant risk. The intensity and risks of a firebrand attack depend on many factors such as the type of vegetation, their ignitability and burning characteristics. The flaming and/or large firebrands have a higher chance to ignite the fuel beds in comparison with glowing and/or small firebrands [15].

Cypress Pine and Red Gum (Figure 2) were used to generate firebrands to assess the influence of the types of vegetation on the effectiveness of the screen. Each vegetation type was mixed to ensure even distribution of wood chip sizes. Preliminary experiments showed that while the vegetation size and shape might differ, the size and shape of generated firebrands were similar.

(**a**) (**b**)

Figure 2. Two types of vegetation used in the study (**a**) cypress pine wood chips, (**b**) red gum wood chips.

Burning too much vegetation increases errors, particularly when no mesh is present, as the likelihood of firebrands hitting the same location on the plastic sheet increases, which causes a miscount in the results as the plastic cannot burn again. Preliminary experiments showed that the use of 0.2 kg vegetation is a good compromise between the required number of firebrands for statistically meaningful results and reducing the

chance of firebrands hitting the same location twice. For a confidence level of 99% and a large population size (Gaussian distribution), the ideal sample size should be 16,577 and 4145 for an error margin of 1% and 2%, respectively. Based on counting the number of generated firebrands in some typical frames of footage of preliminary experiments, 0.2 kg of vegetation has an error margin of 2% and a confidence level of 99% for both vegetation types.

2.3. Combustible Material

The choice of combustible material to be placed at the end of the ESS is critical to accurately assessing the firebrand risk. There are various variables that can affect the survivability of buildings against firebrand exposure. These variables are related to the characteristics of firebrands (e.g., size, vegetation type, ignition temperature), firebrand shower (intensity, duration), ambient conditions (wind speed, temperature, and humidity) and target fuel (material, thickness, direction, temperature, humidity). In this study, the focus is exclusively on quantifying the change in the burning capabilities of flying firebrands during the passage through the mesh. Therefore, the most sensitive material to firebrand shower was desirable. Materials considered include thick and thin plastic, cotton cloth and polyester wadding. Preliminary experiments showed that the 0.02 mm thick polyethylene plastic sheet with a melting point of about 110 °C generates the best outcome. Unfortunately, because the material is so thin, holes in the sheet grow due to the tension force from the wind tunnel. A plastic sheet holder pictured in Figure 3 was manufactured to reduce the tension force. The plastic sheet holder has a solid plate at the back of the plastic sheet and a mesh with 2.5 cm square openings between the plastic sheet and its holder to reduce the tension on the plastic sheet. There is a small distance between the sheet and its holder to minimize the number of firebrands that bounce back after hitting the plastic holder. The plastic sheet still bends in the middle of the openings of the mesh, but the lower tension in the plastic sheet prevents generated holes from tearing instead of burning.

Figure 3. The image of plastic sheet and its holder used in the study.

A low wind speed of less than 4.5 m/s over a fuel bed decreases the ignition time [16]. Preliminary experiments showed that 2 m between the screen and the thin plastic sheet

(or 1.2 m from the end of the wind tunnel) reduces wind speed to 3–4 m/s measured at 10 mm in front of the plastic sheet. As wind speed in this range represents a higher risk of flammability [6,16], 2 m was selected for this study.

The size of the plastic sheet holder was identified during preliminary experiments. If the plastic sheet is too large it impacts the wind speed in the wind tunnel while a small plastic sheet captures fewer firebrands. Many firebrands hit a 58 cm (height) × 24 cm (width) plastic sheet without reducing the wind speed in the wind tunnel.

2.4. Mesh

A stainless-steel mesh (SSWM Bushfire Mesh, SSWOB 01670/USSWOB 0657) with an aperture of 1.67 mm and wire diameter of 0.45 mm with a porosity of 62% which according to the vendor's website [17], complies with the Australian standard for the use in bushfire prone areas. Figure 4 shows the mesh and its frame placed in the mesh holder of the test section of the wind tunnel.

Figure 4. The mesh and mesh frame inside the ESS.

3. Experimental Procedure

The woodchips were dried in the fanned furnace at 110 °C for at least 24 h. Then, the dried vegetation was completely mixed and divided into several 0.2 kg and then each load was placed in the furnace of the ESS. Some kerosene (around 10–20 mL) was splashed on the vegetation to make sure that all vegetation would ignite and burn by the end of each experiment. Figure 5 shows the condition of the furnace before closing the furnace door and turning the fan on. At the end of all experiments, woodchips were only found in the furnace or behind the mesh. Only experiments where less than 1% of the initial woodchip mass remained in said locations were used for the results presented. After placing the plastic sheet in position, the vegetation was ignited and burned for one minute prior to closing the furnace door and turning on the fan. The experiments concluded when no firebrands were observed at the exit for at least one minute. In the end, the plastic sheet was removed for image processing. The area was found by converting the color image to black and white. The number of black pixels was counted and converted to an area in square millimeters. The conversion factor is calculated using 3000 pixels for the 580 mm plastic height resulting in a 26.75 pixels per mm^2 conversion factor. The wind speed in the ESS was measured when the mesh was placed or removed to ensure all experiments were performed at 40 km/h wind speed. For both vegetation types, the temperature of the burning vegetation before closing the furnace door was in the range of 271–275 °C.

Figure 5. Igniting vegetation in the furnace of the ESS.

In total, 50 runs were conducted with (a) 20 preliminary runs to determine the best material and thickness and amount of vegetation to burn, (b) 20 main runs and (c) 10 further runs to confirm hypotheses during post-processing. In all main runs, ambient conditions were recorded, and several cameras were used to record the behaviour of firebrands. The video frames were recorded at 33.3 ms intervals, except if otherwise stated. The duration of each pair of experiments from drying the vegetation to the end of image processing was about two days. The actual run time for each experiment was 5–7 min.

Mesh effectiveness (e) is calculated using the number of holes (e_N) or the area burned (e_A):

$$e_N = 1 - \frac{N_{hole-mesh}}{N_{hole-no\ mesh}} \quad (1)$$

$$e_A = 1 - \frac{\sum A_{hole-mesh}}{\sum A_{hole-no\ mesh}} \quad (2)$$

where the mesh and no mesh subscripts indicate if the mesh was present in the wind tunnel, N is the number of holes and A is the area burned in the plastic sheet by the firebrands.

4. Results

In this section, we start with the analysis of the photographs recorded without the mesh present, then with the mesh present. With the mesh present, eight observed behaviors of the firebrands interacting with the mesh are described with supporting photographs. Then, the photographs and analysis of firebrand behaviors at the distance between the wind tunnel exit and the plastic sheet are presented to ensure the experiment design did not adversely impact the results. Afterwards, as described in the methodology section, the mesh effectiveness is calculated using the images captured of the burned plastic sheets, Equations (1) and (2) and the results are presented. In all photographs, the wind flowed from right to left.

4.1. Visual Observations

4.1.1. Test Section without Mesh

The first runs were conducted using the two types of vegetation without installing the mesh in the wind tunnel. Figure 6a,b shows consecutive frames to demonstrate the firebrand quantity is unsteady in the millisecond time scale. On the scale of seconds, the frequency of firebrands generated is also unsteady. The firebrand lengths are exaggerated in all figures as the firebrands move while the camera shutter is open. The videos showed that the firebrand shower intensity peaked 10–20 s after the start of the runs, remained high

for the first few minutes, and then gradually decreased. Furthermore, note some firebrands hit one of four sides of the wind tunnel (Figure 6a) or the mesh holder (Figure 6b,c) and deflected. Note that no flaming firebrands were observed in the test section due to relatively high wind speed.

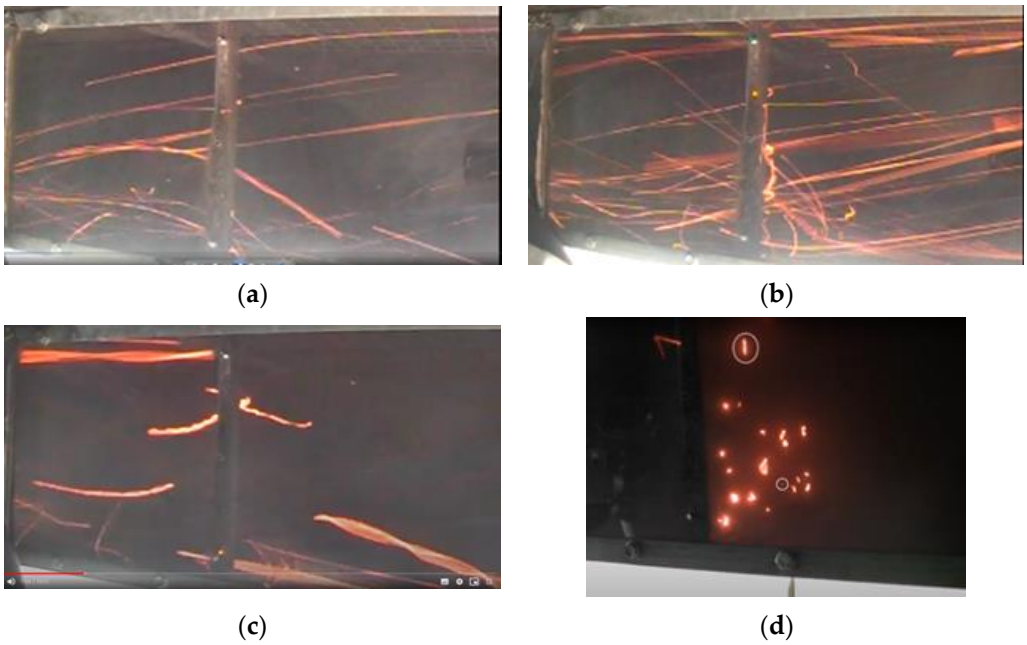

(**a**) (**b**) (**c**) (**d**)

Figure 6. Firebrand shower in the wind tunnel (**a**) low intensity when no mesh was used, (**b**) high intensity when no mesh was used, (**c**) low intensity when no mesh was used, and (**d**) a typical size and shape of firebrands when the mesh was used.

The bottom and top encircled firebrands in Figure 6d show that some of the blocked firebrands are small, and needle-shaped with a cross-sectional area less than the opening of the mesh, respectively.

4.1.2. Test Section with Mesh

Both Cypress and Red Gum firebrands showed similar behaviors when the mesh was placed in the test section except for the higher intensity of the Cypress firebrand shower. The approaching side of the mesh was obviously brighter than the exit side of the mesh (see Figure 15). At the end of most experiments, no firebrands remained at the approaching side of the mesh. In a few runs, some large (>4 mm) and partially burnt firebrands were observed at the end of the experiment. The results of those experiments were excluded, and the runs were repeated. Observations of the firebrands interacting with the mesh are categorized into eight non-exclusive mechanisms which are listed in this section in descending order of occurrence.

- Passing
- Fifty to sixty percent of firebrands passed through the mesh without making contact because the firebrands were smaller, or needle-shaped with a cross-section smaller than the mesh aperture. In Figure 7, (a) a firebrand approaches and (b) passes through the mesh. It should be noted that passing firebrands only appear in one or two consecutive frames while captured firebrands appear in hundreds of consecutive frames. Thus, all photos show more captured firebrands than passing firebrands which may give a false impression.

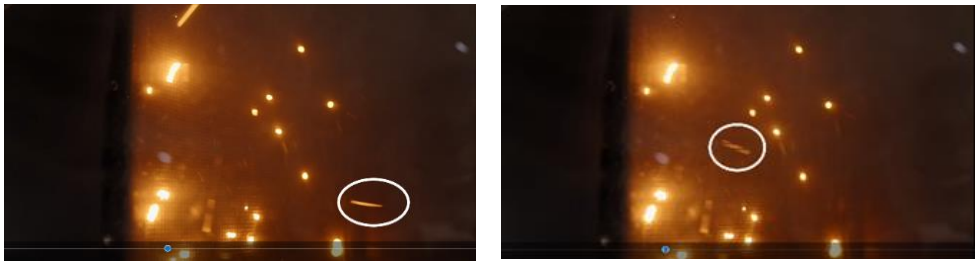

(**a**) (**b**)

Figure 7. A firebrand passes through the mesh without any contact, (**a**) approaching firebrand, (**b**) firebrands after passing the mesh (Stainless Steel Wire and Mesh Pty Ltd. [17]).

- Stopping
- Firebrands hit the mesh and remain stationary behind the mesh at the impact point and continued to burn until quenching and passing through the mesh. In Figure 8, the encircled firebrand is (a) an approaching firebrand, (b) which remained stationary at the hitting point which (c) produced some small secondary firebrands and (d)–(f) reduced size until quenching after 9.68 s, 12.60 s and 12.68 s post impact.

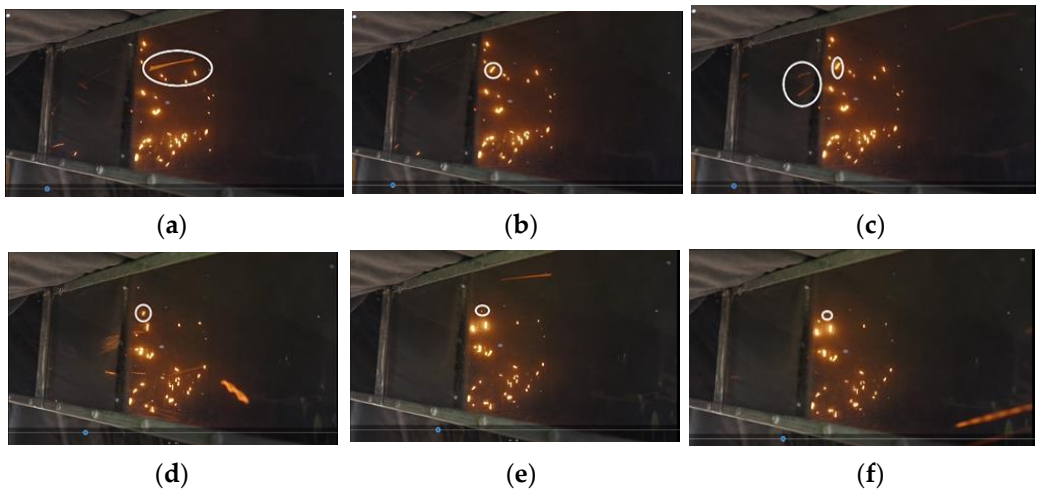

(**a**) (**b**) (**c**)

(**d**) (**e**) (**f**)

Figure 8. Continuation of burning firebrands behind the mesh for 12.68 s. The encircled firebrand shows the state of the firebrand, (**a**) approaching, (**b**) stationary at hitting point, (**c**) producing secondary firebrands, (**d**) 9.68 s after hitting, (**e**) the size diminishing after 12.60 s, and (**f**) after 12.68 s just before quenching (Stainless Steel Wire and Mesh Pty Ltd. [17]).

- Splitting
- In Figure 9, (a) firebrands hit the mesh and (b) split into several smaller firebrands without passing through the mesh.

(**a**) (**b**)

Figure 9. Shows splitting mechanism, (**a**) approaching firebrands, (**b**) firebrands split into three smaller glowing firebrands at approaching side of the screen (Stainless Steel Wire and Mesh Pty Ltd. [17]).

- Shattering
- Firebrands which produce tens of secondary firebrands at the exit side of the mesh after impacting the mesh shown while most of the primary firebrand remains behind the mesh as shown in Figure 10: (a) Two firebrands' approach before (b) impacting the mesh and (c), (d) shatter into tens of secondary firebrands while passing through the mesh.

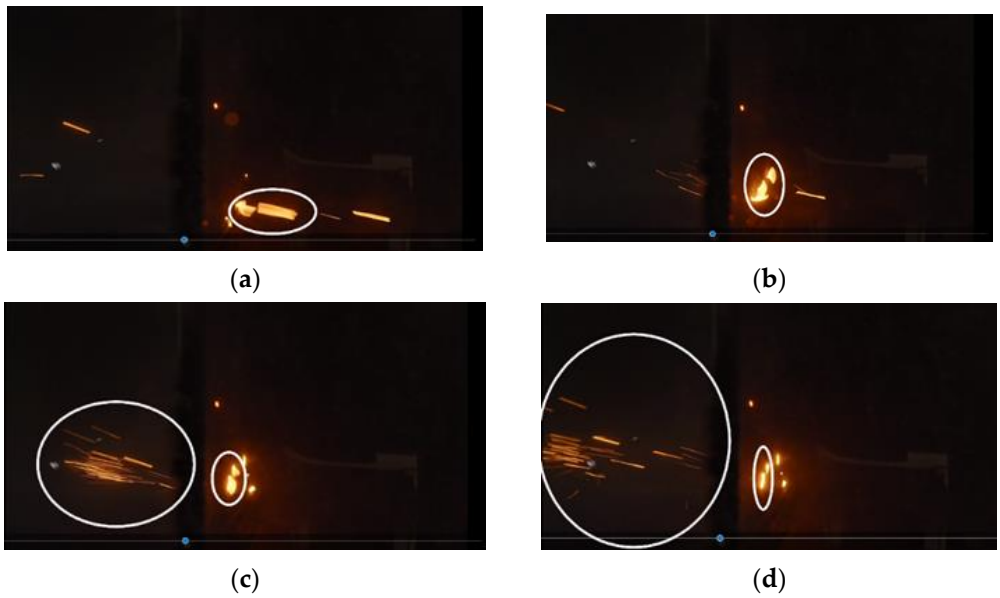

Figure 10. Shattering process, (**a**) two approaching firebrands, (**b**) two firebrands hit the mesh and producing tiny secondary firebrands, (**c**) generated tiny secondary firebrands, and (**d**) movement of tiny secondary firebrands and the change of the sizes of the two original firebrands (Stainless Steel Wire and Mesh Pty Ltd. [17]).

- Pausing
- Firebrands larger than the mesh aperture remain on the mesh, continue to burn until small enough to pass through, sometimes producing tiny secondary firebrands, and the primary firebrand continued burning after passing through. This is shown in Figure 11: (a) A firebrand approaches and (b) impacts the mesh, remains stationary and (c) burns and fragments into two smaller firebrands which later (d) penetrated the mesh.

Figure 11. Firebrands continue to burn before penetrating the mesh, (**a**) approaching the firebrand, (**b**) stopping stationary at the hitting point, (**c**) continuation of burning and fragmentation into two smaller firebrands, and (**d**) penetrating the mesh (Stainless Steel Wire and Mesh Pty Ltd. [17]).

- Bouncing
- Firebrands hit the mesh and bounce back (Figure 12), which due to high wind speed within the wind tunnel, return and hit the mesh again which caused some firebrands to fragment into smaller pieces.

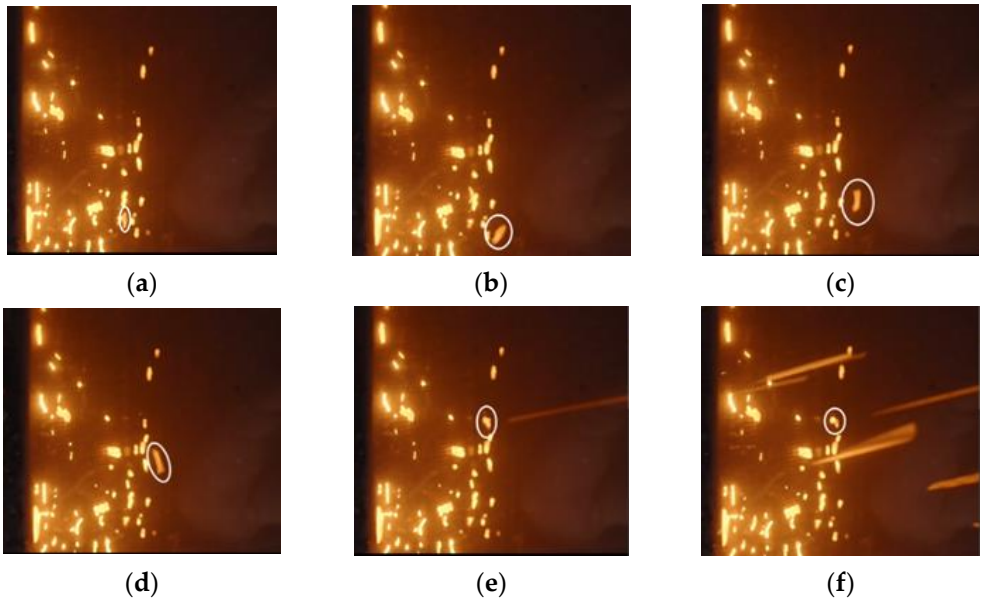

Figure 12. Firebrands bounce back after hitting the mesh. The encircled firebrands (**a**) impact the mesh, (**b**) bounce back, (**c**–**e**) return to the mesh and (**f**) settle into a new position and continue to burn (Stainless Steel Wire and Mesh Pty Ltd. [17]).

- Slipping
- A small percentage of firebrands hit the mesh and slip across the mesh (Figure 13). Some slipping firebrands produce tiny secondary firebrands during their movement.

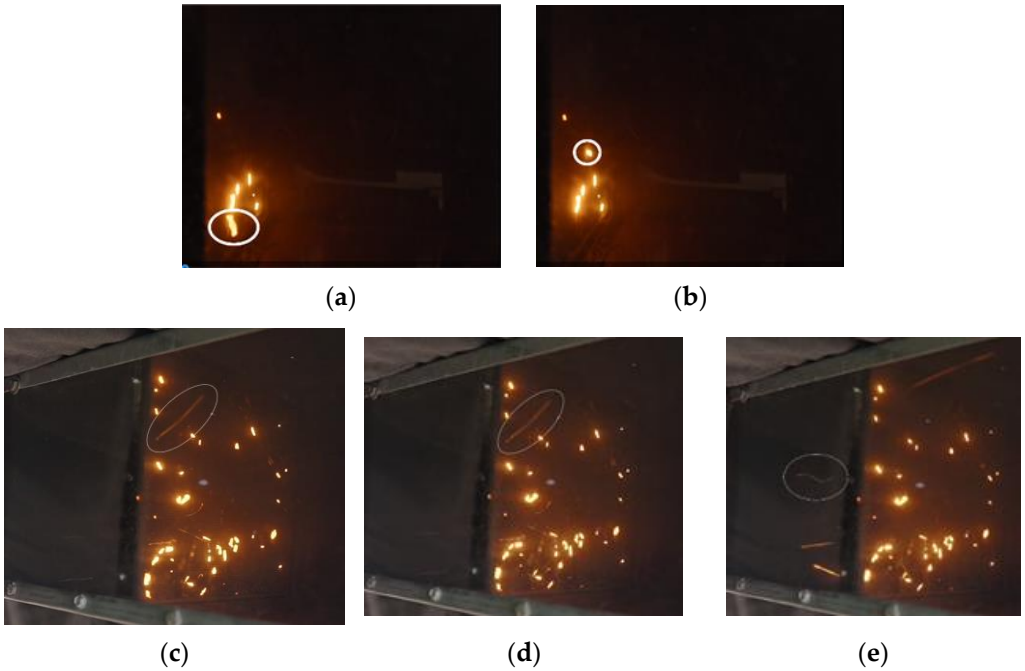

Figure 13. The slipping firebrands, (**a**) a firebrand at hitting point, (**b**) the firebrand slipped and changed and became a pausing firebrand, (**c**) an approaching firebrand, (**d**) the slippage of the firebrand, (**e**) the firebrand became quenched at its new location and passed (stopping firebrand) (Stainless Steel Wire and Mesh Pty Ltd. [17]).

- Wandering
- At the exit side of the mesh, some small firebrands were trapped between low- and high-pressure regions produced in the wake of the mesh. These firebrands stayed

behind the mesh with some random movements and were mostly quenched as they were small. Figure 14a–h show one of these firebrands at consecutive frames.

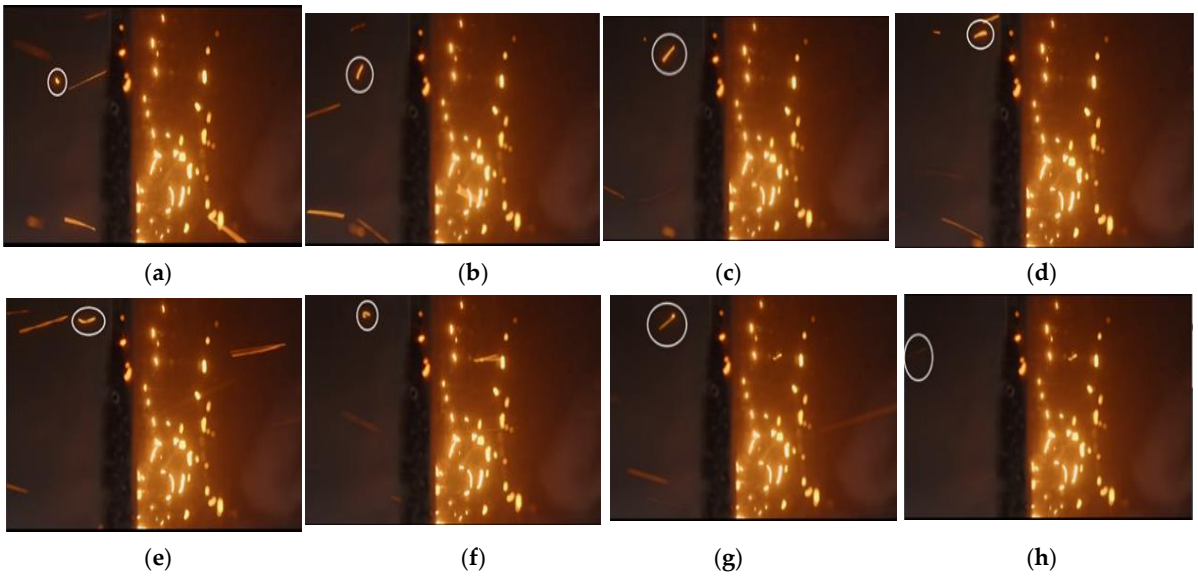

Figure 14. Wandering of small firebrands at the exit side of the mesh in consecutive frames of (**a**–**g**) shows the end of wandering and movement in wind direction, (**h**) shows the firebrand quenched (Stainless Steel Wire and Mesh Pty Ltd. [17]).

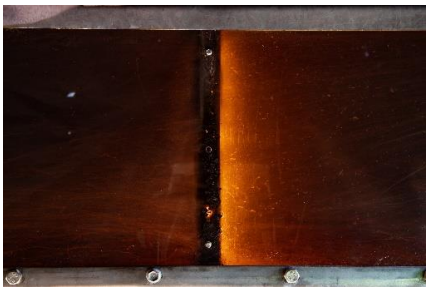

Figure 15. The approaching side (**right**) is brighter than exit side (**left**). (Stainless Steel Wire and Mesh Pty Ltd. [17]).

Figure 16a appears to show firebrands with a cross-section greater than the mesh aperture passing through the mesh. At an earlier time, shown in Figure 16b, the firebrand had a needle shape which allowed it to penetrate the mesh because its cross section was smaller than the mesh aperture, as it turned and moved in a direction normal to its length.

Figure 16. Deceivingly large firebrands at the exit side of the mesh taken by a camera with a speed of 250 frames per second (**a**) a firebrand with an apparent cross-section greater than the opening of the mesh at the exit of the mesh, and (**b**) the previous frame shows the of the actual needle shape of the firebrand in a). (Stainless Steel Wire and Mesh Pty Ltd. [17]).

4.1.3. At the Exit of the Wind Tunnel

Large firebrands captured by the mesh produced many tiny secondary firebrands. Photographs and videos show the mesh resulted in significantly fewer penetrated glowing firebrands with instead many small and quenched firebrands at the exit of the wind tunnel. This is depicted in Figure 17 with photographs taken with a 4 ms shutter time. Figure 17a shows eight quenched firebrands (encircled white), five firebrands almost quenched (encircled yellow) and one glowing firebrand (encircled red) when the mesh was used. Figure 17b,c shows a needle-shaped firebrand. Without mesh, both small and large glowing or quenched firebrands were present, but the ratio of glowing to quenched firebrands was greater than with the mesh. Figure 17d shows the number and size of glowing firebrands were higher and larger as they exited the wind tunnel before impacting the plastic sheet. Occasionally some enormous firebrands (see Figure 17e) were observed.

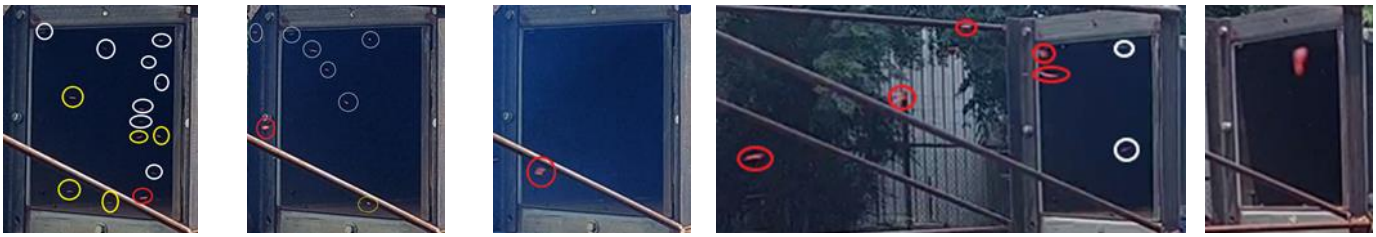

(**a**) (**b**) (**c**) (**d**) (**e**)

Figure 17. Firebrands at the exit of the wind tunnel. White, yellow and red circles show quenched, almost quenched and glowing firebrands. All photos taken with a camera set for a shutter speed of 4 milliseconds. The mesh was placed in the test section for (**a**–**c**) and no mesh was used for (**d**,**e**).

4.1.4. At the Plastic Sheet

The images show the size of the plastic sheet is adequate to be exposed to most firebrands exiting the wind tunnel, both with and without the mesh present. There were considerably fewer glowing firebrands hitting the plastic sheet with the mesh present (see Figure 18). Despite all efforts, the videos show some holes are larger than the area of the burning part of the firebrands due to the slippage of some firebrands on the plastic sheet, the vibration of the plastic sheet and continuation of the burning of the firebrands.

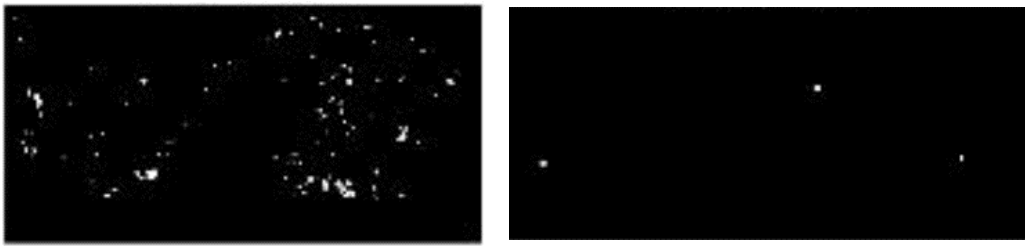

(**a**) (**b**)

Figure 18. The image of plastic sheet and generated holes after image processing, (**a**) no mesh was used (experiment 19 in Table 1), (**b**) mesh was used (experiment 20 in Table 1).

The simplified effectiveness calculated by Equations (1) and (2) is lower than the actual effectiveness for two reasons. First, most firebrands, particularly smaller firebrands, are bound to the plastic sheet and continued to burn to create holes usually equal to or larger than the size of the burning part of the firebrands (the higher numerator in Equation (2)). However, a small fraction of large firebrands particularly those hitting the sheet from their unburnt side bounced back after the hitting, therefore the holes were smaller than the burning area of firebrands (the lower denominator in Equation (2)). Therefore, the calculated efficiency from Equation (2) is expected to be less than the actual value. Second, as more holes (as shown in Figure 18) are burned without the mesh, the chance of two or

more firebrands hitting the same hole is higher (lower denominator than actual value in Equation (1)). Therefore, it is expected the calculated effectiveness ratios of the mesh based on Equations (1) and (2) will be lower than the actual values.

Considering around 50% to 60% of firebrands passed through the mesh, it was expected to see small size holes on the plastic sheet in most experiments with the mesh while there were many small holes when the mesh was not used. There is no evidence that without mesh the small holes formed due to fragmentation of large firebrands.

4.2. Mesh Effectiveness

The ambient conditions and the number of holes and their total sizes on the thin plastic sheet exposed to Red Gum and Cypress firebrands shower for 20 experiments with and without placing the mesh in the test section are presented in Table 1. The number of holes was counted, and their total area was calculated using a script. Table 1 shows the number of holes without mesh ranged from 13 to 77 and 85 to 125 for Red Gum and Cypress respectively. This difference is due to about 30% greater density of Red Gum than Cypress at 965 kg/m^3 and 680 kg/m^3, respectively, [18]. The lower density of Cypress woodchips indicates a higher volume of cypress woodchips for the same mass, and Cypress wood chips would be lighter than Red Gum for a given size. The number of holes significantly decreased to 1–3 for red gum and 0–4 for cypress firebrands when the mesh was placed in the test section. The use of mesh decreased the total area of holes in the range of 582–1390 mm^2 for red gum and 3037–9021 mm^2 for Cypress to the range of 3–121 mm^2 for Red Gum and 0–163 mm^2 for Cypress.

Table 1. The numbers of holes created by 0.2 kg firebrands of red gum woodchips at a wind speed of 40 km/h on a plastic sheet of 0.02 mm thickness with and without the stainless-steel mesh with an aperture of 1.67 mm and wire diameter of 0.45 mm which represents a porosity of 62%. minimum, average and maximum hole area on the plastic sheet at the end of experiments.

Run	Vegetation	$T_{ambient}$ (°C)	$\phi_{ambient}$ (%)	Mesh Used?	N_{holes}	ΣA_{holes} (mm^2)	Min. A_{hole} (mm^2)	Ave. A_{hole} (mm^2)	Max. A_{hole} (mm^2)	e_N (%)	e_A (%)
1	Red Gum	30	39	No	18	923	0.3	51.3	557		
2		30	38	Yes	2	11	2.7	5.5	8.3	89%	99%
3		30	42	No	13	582	0.8	44.8	194		
4		30	40	Yes	1	3	3	3	3	92%	99%
5		30	40	No	77	1390	0.04	18.1	133		
6		29	38	Yes	3	47	8	15.7	22	96%	97%
7		30	39	No	49	1351	2.4	27.6	149		
8		30	37	Yes	3	121	26	40.3	55	93%	91%
9		28	46	No	28	1125	0.4	40.2	146		
10		27	54	Yes	1	87	87	87	87	96%	92%
Overall effectiveness of the mesh against red gum firebrands at wind speed of 40 km/h										93.2% ± 2.8%	95.6% ± 3.5%
11	Cypress	27	55	No	85	3037	0.64	35.7	178		
12		28	53	Yes	0	0	0	0	0	100%	100%
13		31	35	No	93	3423	0.04	46.8	149		
14		27	53	Yes	0	0	0	0	0	100%	100%
15		30	33	No	111	9021	0.71	81.3	1587		
16		28	53	Yes	3	163	0.15	54.3	113	97%	98%
17		30	34	No	125	6684	1.4	53.5	1515		
18		27	51	Yes	4	19	3.0	4.75	7.6	97%	99%
19		28	47	No	85	3098	3.7	36.4	283		
20		26	56	Yes	3	104	20.7	34.7	47	96%	97%
Overall effectiveness of the mesh against Cypress firebrands at wind speed of 40 km/h										98.0% ± 1.7%	98.8% ± 1.2%

The effectiveness was calculated using Equations (1) and (2). Despite the large range in the number of holes and the total area between runs, there was only a 3.5% maximum standard deviation for the effectiveness. The hole effectiveness e_N is 89–96% for Red Gum firebrands and 96–100% for Cypress firebrands. The area effectiveness e_A is 91–99% for Red Gum embers and 97–100% for Cypress firebrands. For both e_N and e_A the mesh performed slightly better for Cypress firebrands. The average hole effectiveness (e_N) is 93.2% against Red Gum embers and 98.0% against Cypress firebrands. The average area effectiveness (e_A) is slightly higher at 95.6% and 98.8% for Red Gum and Cypress firebrands respectively. In all cases, the mesh performed slightly better against Cypress firebrands compared to Red Gum firebrands. Table 1 also shows the maximum, average and minimum sizes of the holes on the plastic sheet. As expected, the mesh reduced the maximum hole area in all runs. The large size of the holes on the plastic sheet (e.g., 113 mm^2 for run 16) when the mesh was used is due to the penetration of needle shape firebrands through the mesh.

Table 1 shows the average size of holes reduced when the mesh was used except for runs 8 and 10. The photos of plastic sheets show the many small holes in no mesh runs (e.g., see Figure 18a) which reduced the average size of holes. Table 1 confirms that except for runs 15 and 16, the smallest holes were smaller in no mesh experiments. This indicates that the mesh blocks many small and large firebrands except for a few needle shape firebrands. Furthermore, most penetrated firebrands and tiny secondary firebrands produced by the mesh were not able to burn the plastic sheet, as shown by the 0.15 mm^2 minimum hole area in experiment 16, but given how often firebrands quench at the wind tunnel exit the risk associated with small firebrands is minimal.

5. Discussion

The most important parameters affecting the results were controlled and included mass and the size distribution of woodchips, wind speed in the wind tunnel and amount of kerosene used to ignite woodchips. However, ambient conditions and turbulence in the furnace were not fully controlled and may have contributed to the fluctuations in the results. Despite the above-uncontrolled variables and the stochastic nature of the experiment, the standard deviation of experiments was 1.2–3.5% which shows the reliability of the results.

Under the conditions of the experiments, the descending order of the observed behaviors of firebrands interacting with the mesh were passing, stopping, splitting, shattering, pausing, slipping, bouncing, and wandering. It was observed that about 50–60% of the firebrands passed through the mesh without any contact (or a noticeable contact). The passage of more than 50% of firebrands through the mesh raises a question about the accuracy of the minimum area of holes presented in Table 1.

It was expected to see the minimum size of holes to be comparable between mesh and no mesh cases for a high passing ratio, but except for experiment 16, the results show that the minimum size of holes is considerably greater when the mesh was used. This can be explained by probability theory. In Figure 19, the center of the passing firebrand can be at any point in the square of ABCE (cell) when no mesh was used. With mesh, the center of the passing firebrand can only be in the square of FGHI. Strictly, the stagnation region in front of the wire means the probability that the center of the firebrand is found anywhere within the cell is non-uniform, but making this simplification, the probability of the passage of the firebrand ($P_{passing}$) through the mesh is the ratio of the area of FGHI (S_{FGHI}) to the area of ABCE (S_{ABCE}):

$$P_{passing} = \frac{S_{FGHI}}{S_{ABCE}} = \frac{(a-d)^2}{(a+D)^2} \quad (3)$$

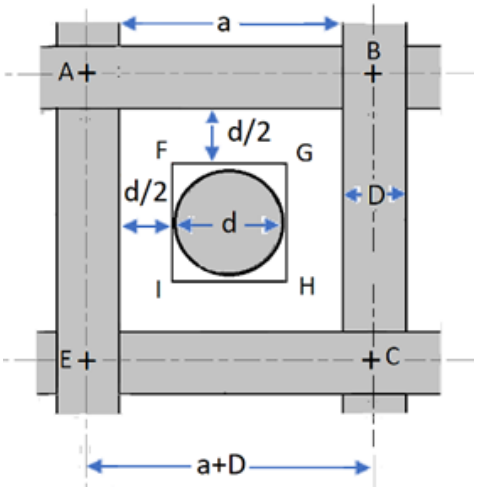

Figure 19. Passage of firebrand with a diameter *d* through a screen with wire diameter *D* and aperture *a*.

The probability of a circular firebrand with a diameter of 0, 0.5 mm, 1 mm, and 1.5 mm passing through a 1.67 mm aperture mesh with a 0.45 mm diameter is 62%, 30%, 10% and 0.6%, respectively, using Equation (3). In other words, the mesh blocks 100% of circular firebrands with a diameter of greater than 1.67 mm, 99.4% of circular firebrands with a diameter of 1.5 mm, 90% of circular firebrands with a diameter of 1 mm, 70% of circular firebrands with a diameter of 0.5 mm and 38% (1-porosity) of circular firebrands with a diameter of zero.

The passing small firebrands and tiny secondary firebrands produced by the mesh (mostly due to shattering) were either quenched before exiting the wind tunnel (see Figure 17a) or did not burn the plastic sheet in most cases (see Figure 18b).

Firebrands show one or a combination of eight behaviors when interacting with the mesh. The impact of the eight behaviors on the effectiveness of the mesh varies. The most positive behavior is stopping as firebrands completely quench. Shattering is also useful as it slices large firebrands into many tiny secondary firebrands which are unlikely to pose any risk. Passing is the least positive behavior as the chance of the passage of firebrands with a size comparable to the aperture of the mesh is not zero. In addition, firebrands with small cross-sections but long lengths have some chance of passing. Therefore, the effectiveness of the mesh is expected to decrease if the firebrand shower consists of more needle shape firebrands with small cross-sections. Shattering is expected to occur more frequently at higher wind speeds or for more fragile firebrands. Larger firebrands are more likely to exhibit stopping and pausing behaviors and less likely to exhibit passing and wandering behaviors. The effectiveness can change due to wind speed, type of vegetation and size of firebrands. This study only documented the slight impact of the type of vegetation on the effectiveness.

The calculated effectiveness ratios are only indicative of real wildfires due to unsteady wind speed, combinations of different types of vegetation, and variable distance between where the firebrands ignite and contact with the mesh during a real firebrand attack. In the wind tunnel experiment, the sizes of firebrands are expected to be smaller than the firebrands in a real wildfire due to high turbulence in the furnace and possible collision with the sides of the wind tunnel. Therefore, higher effectiveness ratios are expected for larger mesh in the wind tunnel as it increases the hydraulic diameter of the test section and therefore less collision occurs. In real wildfires, the intensity of the firebrand shower could differ from the results shown here. It is expected that the penetration ratio will decrease, and effectiveness will increase as a higher proportion of firebrands block more openings of the mesh during a firebrand shower. In the wind tunnel experiments, the firebrand has no path except to pass through the mesh. In real wildfires, low porosity meshes generate a

stagnation zone before the mesh causing the firebrands to pass around the mesh causing a ninth behaviour of the firebrand and mesh interaction, "deflection".

Two limitations should be considered when interpreting the results of this study. First, this study focused on comparing the burning capabilities of firebrands with and without mesh on a sensitive plastic sheet. In real-world conditions, the number and intensity of firebrands approaching the target fuel are important. Therefore, while the high effectiveness of the mesh was measured, this study did not explore the minimum intensity of firebrands capable of burning target fuels. The intensity of firebrands on target fuel can easily change by changing the initial intensity. Second, this study did not consider several variables such as type, thickness and direction of target fuel beds and ambient conditions which are expected to influence the minimum intensity required to burn the fuel beds.

Measuring the effectiveness of the mesh by a vertical thin plastic sheet gave reliable results however a possible improvement to reduce the miscounts associated with firebrands impacting the same position on the plastic sheet twice would be to move the plastic sheet using a low-speed motor.

6. Conclusions

The aim of the research was to quantify the effectiveness of a mesh with an aperture size of 1.67 mm and wire diameter of 0.45 mm at a wind speed of 40 km/h against a firebrand shower. Two effectiveness ratios were defined based on the ratio of the number of holes and the sum of areas of holes created by the firebrand shower on a vertical thin plastic sheet which was placed 2 m away from the test section with and without placing the mesh in the test section. Two types of vegetation of 0.2 kg Red Gum and 0.2 kg Cypress woodchips were burned in the UniSQ Ember Shower Simulator (ESS) to produce firebrands for 5–7 min. Due to the stochastic nature of the experiments, the experiments were repeated five times for each type of vegetation, with and without the mesh, for a total of 20 experiments. The technique of exposing a vertical thin plastic sheet to a firebrand shower was effective to quantify the effectiveness of the mesh but there is room for improvement.

The duration of the experiments could not have been increased due to the possibility of double hitting a hole by several firebrands. Similar behaviors were observed for both vegetations. Firebrands showed one or more of eight different behaviors around the mesh. The most frequently observed behavior was passing through the mesh without any contact. Most of the passing firebrands were very small and were quenched before reaching the exit of the wind tunnel or were not able to burn the thin plastic sheet. The second most observed behavior was stopping. Firebrands were captured by the mesh and continued to burn until quenching and then passing through the mesh. The third common behavior was splitting. The firebrands split into two or more glowing firebrands at the approaching side of the mesh. The fourth most common behavior was shattering which was a positive mechanism as the sizes of produced secondary firebrands were tiny and very unlikely to pose any risk. The fifth behavior is pausing where captured firebrands continued to burn until fitting the openings of the mesh and then downsized glowing firebrands penetrated the mesh. The three other positive behaviors are slipping, bouncing, and wandering. These mechanisms were useful as they gave time to burning firebrands to quench or downsize during these processes. The largest holes were caused by needle-shaped firebrands (with a cross-section smaller than the mesh aperture) due to their larger mass.

The effectiveness of the mesh defined based on the number of holes under the conditions of the experiments were 93.2 $\pm$ 2.8% and 98.0 $\pm$ 1.7% for Red Gum and Cypress firebrands, respectively. The effectiveness of the mesh defined based on the area of holes were 95.6 $\pm$ 3.5% and 98.8 $\pm$ 1.2% for Red Gum and Cypress firebrands, respectively. The results show that the mesh is highly effective in reducing risks associated with Red Gum and Cypress firebrands 2 m from the mesh at a wind speed of 40 km/h under conditions of the experiments except for long needle shape firebrands, but they are not able to provide full protection.

Author Contributions: A.S.B.; Conceptualization, methodology, validation, formal analysis, investigation, resources, data curation, original draft preparation, visualization, supervision, project administration, funding acquisition. M.d.P.; methodology, software, validation, formal analysis, investigation, resources, data curation, writing—review and editing, visualization. All authors have read and agreed to the published version of the manuscript.

Funding: This research was funded under a sponsored research agreement (contact USQ1049262021, Project 1007952) between the University of Southern Queensland (UniSQ) and Stainless Steel Wire & Mesh Pty Ltd. (SSWM), 3 Commercial Court, Tullamarine VIC 3043, Australia.

Institutional Review Board Statement: Not applicable.

Informed Consent Statement: Not applicable.

Data Availability Statement: The data presented in this study are available on request from the corresponding author. The data are not publicly available due to the large video file sizes.

Conflicts of Interest: The funders had no role in the design of the study; in the collection, analyses, or interpretation of data; in the writing of the manuscript; or in the decision to publish the results.

References

1. Standards Australia. Construction of Buildings in Bushfire Prone Areas AS 3959:2018. *SAI Global*. Available online: https://infostore.saiglobal.com/en-au/search/standard/?searchTerm=AS%203959:2018&productFamily=STANDARD&q=AS%203959%3A2018 (accessed on 28 May 2022).
2. Manzello, S.L.; Shields, J.R.; Yang, J.C.; Hayashi, Y.; Nii, D. On the use of a firebrand generator to investigate the ignition of structures in wildland-urban interface (WUI) fires. In Proceedings of the 11th International Conference on Fire Science and Engineering (INTERFLAM), London, UK, 3–5 September 2007; Interscience Communications Ltd.: London, UK, 2007.
3. Manzello, S.L.; Hayashi, Y.; Yoneki, Y.; Yamamoto, Y. Quantifying the vulnerabilities of ceramic tile roofing assemblies to ignition during a firebrand attack. *Fire Saf. J.* **2010**, *45*, 35–43. [CrossRef]
4. Hashempour, A.J. Investigating Potential of Metal Mesh to CONTAIN wildfires. Ph.D. Thesis, University of Southern Queensland, Toowoomba, Australia, 2017.
5. Sharifian, A.; Hashempour, A.J. A novel ember shower simulator for assessing performance of low porosity screens at high wind speeds against firebrand attacks. *J. Fire Sci.* **2016**, *34*, 335–355. [CrossRef]
6. Sharifian, A.; Hashempour, A.J. Wind tunnel experiments on effects of woven wire screens and buffer zones in mitigating risks associated with firebrand showers. *Aust. J. Mech. Eng.* **2018**, *18*, 156–168. [CrossRef]
7. Manzello, S.L.; Cleary, T.G.; Shields, J.R.; Yang, J.C. On the ignition of fuel beds by firebrands. *Fire Mater.* **2006**, *30*, 77–87. [CrossRef]
8. Manzello, S.L.; Cleary, T.G.; Shields, J.R.; Maranghides, A.; Mell, W.E.; Yang, J.C. Experimental Investigation of Firebrands: Generation and Ignition of Fuel Beds. *Fire Saf. J.* **2008**, *43*, 226–233. [CrossRef]
9. Bahrani, B. *Characterization of Firebrands Generated from Selected Vegetative Fuels in Wildland Fires*; The University of North Carolina: Charlotte, NC, USA, 2020.
10. Wickramasinghe, A.; Khan, N.; Moinuddin, K. Determining Firebrand Generation Rate Using Physics-Based Modelling from Experimental Studies through Inverse Analysis. *Fire* **2022**, *5*, 6. [CrossRef]
11. Sardoy, N.; Consalvi, J.L.; Porterie, B.; Fernandez-Pello, A.C. Modeling transport and combustion of firebrands from burning trees. *Combust. Flame* **2007**, *150*, 151–169. [CrossRef]
12. Manzello, S.L.; Suzuki, S.; Gollner, M.J.; Fernandez-Pello, A.C. Role of firebrand combustion in large outdoor fire spread. *Prog. Energy Combust. Sci.* **2020**, *76*, 100801. [CrossRef] [PubMed]
13. Wells, R.W. *Fire at Peshtigo*; Prentice-Hall: Englewood Cliffs, NJ, USA, 1968.
14. Chandler, C.; Cheney, P.; Thomas, P.; Trabaud, L.; Williams, D. *Fire in Forestry*; John Wiley and Sons: New York, NY, USA, 1983.
15. Manzello, S.L.; Cleary, T.G.; Shields, J.R.; Yang, J.C. Ignition of mulch and grasses by firebrands in wildland-urban interface fires. *Int. J. Wildland Fire* **2006**, *15*, 427–431. [CrossRef]
16. Ganteaume, A.; Lampin-Maillet, C.; Guijarro, M.; Hernando, C.; Jappiot, M.; Fonturbel, T.; Pérez-Gorostiaga, P.; Vega, J.A. Spot fires: Fuel bed flammability and capability of firebrands to ignite fuel beds. *Int. J. Wildland Fire* **2009**, *18*, 951–969. [CrossRef]
17. Stainless Steel Wire and Mesh (SSWM), Bush Fire Mesh (BFM) SSWOB 01670 Steel. Available online: https://www.sswm.com.au/bushfiremesh/PDF-Documents/Bushfire-Mesh/SSWOB-01670-BM.pdf (accessed on 4 August 2022).
18. Government of Western Australia, Forest Products Commission, Species Information. Available online: https://www.wa.gov.au/system/files/2020-09/FPC-species-information.pdf (accessed on 4 August 2022).